Minireview

Luminescent gold nanoparticles: A new class of nanoprobes for biomedical imaging

Chen Zhou, Shengyang Yang, Jinbin Liu, Mengxiao Yu and Jie Zheng

Department of Chemistry, The University of Texas at Dallas, Richardson, TX 75080, USA
Corresponding author: Jie Zheng. Email: jiezheng@utdallas.edu

Abstract

Our fundamental understanding of cell biology and early diagnosis of human diseases have been greatly benefited from the development of fluorescent probes. Over the past decade, luminescent gold nanoparticles (AuNPs) with diverse structural parameters including particle size, surface ligands, valence state and grain size have been synthesized and have begun to emerge as a new class of fluorescent probes for bioimaging because of their great biocompatibility, robust photophysical properties and tunable emissions from the visible range to the near infrared region. In this minireview, we summarize the recent progress in applications of different-sized luminescent AuNPs as imaging probes for both *in vitro* and *in vivo* levels.

Keywords: Luminescent, gold, nanoparticles, bioimaging

***Experimental Biology and Medicine* 2013; 238: 1199–1209. DOI: 10.1177/1535370213505825**

Introduction

Bioimaging techniques and related contrast agents have greatly advanced our fundamental understanding of cell biology and also make it feasible to achieve earlier diagnosis of many diseases.[1,2] Low-cost, portable and noninvasive fluorescence imaging is one of such techniques widely used in molecular imaging applications at both in vitro and in vivo levels.[3–6] To enhance the contrast of fluorescence-based imaging techniques, a large number of fluorescent probes ranging from organic dyes to fluorescent proteins and quantum dots (QDs) have been developed.[7–13] However, each type of fluorescent probes has its own strengths and limitations. For example, as the most widely used probes, small organic dyes such as cyanine dyes exhibit bright and tunable emission from blue to near infrared (NIR).[14,15] Since organic fluorophores often exhibit low interference on the binding affinities and dynamics of labelled biological molecules, they have been extensively used in studying distributions of biomolecules of interest, probing conformational dynamics of proteins and unravelling complicated cellular structures at both ensemble and single molecule level.[16,17] In addition, many organic dyes also serve as contrast agents to image tumours and other diseases or as indicators to report local biochemical environment at the in vivo level.[18–20] More recently, these merits of small organic probes also lead to new breakthroughs in bioimaging including super-resolution fluorescence microscopy and fluorescence-guided cancer surgery.[21,22] While organic dyes have found broad bioimaging applications, a lack of specificity for any particular protein and low permeability to the cell membrane often limit their applications to fixed or permeabilized cells.[12]

The emergence of fluorescent proteins not only successfully addresses these challenges but also revolutionizes the cell imaging by allowing realtime correlation of protein functioning with biochemical processes in live cells.[23,24] Green fluorescent protein and its variants with different emissions can be readily fused to any protein of interest.[25,26] This unique advantage of fluorescent proteins allows us to quantify individual or multiple protein species, probe protein–protein interactions and track the fate of specific protein populations in realtime within the complex environment of the cells.[12,27] While these genetically encodable fluorophores offer unprecedented opportunities for bioimaging, their photobleaching and low-emission intensities preclude them from many other imaging applications that are involved with long-term tracking and high-temporal studies.[12]

Semiconductor QDs exhibit bright, robust and size-dependent emissions, successfully addressing the long-stand challenges in photostability and brightness that organic fluorophores and fluorescence proteins face.[28,29] These merits of QDs in optical properties further extend biomedical application of fluorescence imaging techniques. In the past decades, QDs not only have found broad applications in conventional immunofluorescence assays, fluorescence in situ hybridization, cell and animal imaging by greatly enhancing signal-to-background ratios, but also led to the emergence of new imaging approaches such as three-dimensional (3D) optical sectioning, correlated fluorescence-electron microscopy

and multiplexing imaging.[9,11,30–34] However, the large particle size, complex surface chemistry and potential leaching of toxic metal ions from QDs often limit their applications to in vitro diagnosis, permeabilized cells, extracellular or endocytosed proteins, and in vivo animal imaging.[35–38]

While noble metal nanoparticles (NPs) have found broad applications in bioimaging, they are seldom considered as fluorophores for bioimaging. Indeed, conventional metal NPs are not fluorescent because of their extremely large density of states.[39] Under the light excitation, collective oscillation of free electrons rather than single-electron transitions is induced; therefore, surface plasmons rather than fluorescence are observed. Over the past decade, significant efforts have been devoted to develop luminescent metal NPs, which can give intrinsic emissions without conjugation of additional fluorophores.[40–42] Luminescent gold nanoparticles (AuNPs) with size ranging from 0.3 to 20 nm have been synthesized by tuning various structural parameters including particle size, surface ligands, valence state and grain size.[43] Generally, different-sized luminescent AuNPs can be classified into molecular luminescent AuNPs and plasmonic luminescent AuNPs, in which molecular AuNPs can be further divided into two subclasses: few-atom Au nanoclusters (AuNCs) and few-nm AuNPs (Scheme 1). In these luminescent AuNPs, the molecular luminescent AuNPs generally are lack of the characteristic surface plasmon of conventional AuNPs due to the limited number of free electrons, but can give a broad range of emissions from visible to NIR regions, while both luminescence and surface plasmon can be attained within single plasmonic luminescent AuNPs by tuning grain size of NPs.[43] Although these newly developed luminescent AuNPs have not yet as widely applied as conventional organic dyes or semiconductor QDs in bioimaging, their biocompatibility, physiological stability, facile synthesis process and diverse photophysical property make them very promising candidates. In this minireview, we present the synthetic strategies for creating different-sized luminescent gold NPs and summarize their applications in the biomedical imaging at both in vitro and in vivo levels.

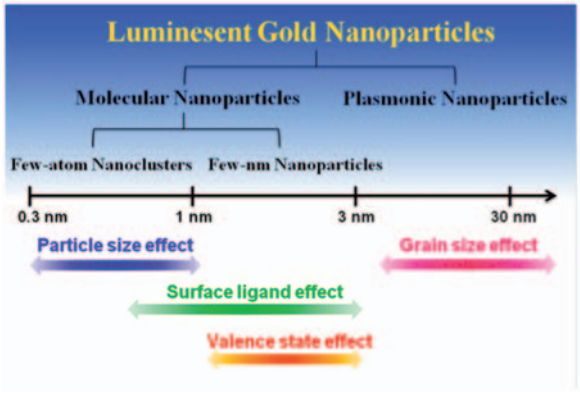

Scheme 1 Luminescent AuNPs can be divided into two major classes: molecular NPs and plasmonic NPs. For molecular NPs, they can be further divided into two subclasses: few-atom nanoclusters and few-nm NPs, where particle size, surface ligands and valence states all have significant impacts on their luminescence properties. For plasmonic NPs, grain size plays a key role in the emission. (Reprinted from Ref. 43, with permission from Royal Society of Chemistry.) AuNCs: gold nanoclusters; NPs: nanoparticles. (A colour version of this figure is available in the online journal)

Few-atom luminescent AuNCs

Electronic structure of a single AuNP is dependent on its particle size.[44] When particle size is close to electron Fermi wavelength of gold metal (0.5 nm), continuous band structure of the NPs breaks into discrete energy states, which fail to support surface plasmon but result in molecular-like electronic transition.[45,46] On this extremely small size scale, AuNPs are often denoted as AuNCs, whose behaviour is expected to bridge a link between gold atoms and large AuNPs.[47–49]

Dendrimers are often employed in the synthesis of monodisperse AuNCs. For example, poly-amidoamide (PAMAM) dendrimers are utilized for their tertiary amine groups at the branching points within the dendrimer.[50] When introduced to the aqueous dendrimer solution, gold ions generally form a complex with the lone pair of electrons present at the tertiary amines. After complexation, the ions are reduced to form NCs that are encapsulated within the dendrimers. By using PAMAM dendrimer as template, luminescent AuNCs with quantum yield up to 70% were successfully synthesized.[51] The fluorescence emission of the AuNCs can be finely regulated from the visible range to the NIR region (Figure 1a) by tuning the molar ratio of dendrimers to gold salts.[49] In these cases, the emission energy of AuNCs is totally dependent on the number of gold atoms (N) in each AuNC and coincides with a simple scaling relation of $E_{Fermi}/N^{1/3}$, in which E_{Fermi} is the Fermi energy of bulk gold (5.53 eV). As seen from Figure 1b, the electronic structure of dendrimer coated few-atom AuNCs is determined by the number of free electrons in AuNCs, in accordance with a free-electron (Jellium) model.[52–54] In addition, following a similar procedure illustrated above, diverse luminescent AuNCs with different emissions can be also synthesized by coating with various ligands, including polyethylenimine, glutathione (GSH), poly(N-vinylpyrrolidone), bovine serum albumin (BSA), pepsin and other molecules.[55–62]

In vitro fluorescence imaging of few-atom luminescent AuNCs

The receptor-mediated internalization of AuNCs by cells had been observed by Lin et al.[63] in 2008, where AuNCs functionalized with nuclear-specific leading peptide SV40 NLS can enter both the cytoplasm and nucleus of living HeLa cells after 1.5-h treatment. In addition, a nonspecific pathway that AuNCs were internalized in cells was also observed by Jao et al.[64] They found that the positively charged dendrimer-encapsulated blue-emitting Au_8 cluster core was able to penetrate into the HeLa cells due to the electrostatic interactions with cell membrane and were predominantly localized in the cytoplasm, while AuNCs coated with neutral charged dendrimer cannot be internalized. NIR-emitting AuNCs minimize autofluorescence interference and phototoxicity, further broadening the bioimaging applications of few-atom luminescent AuNCs.[65,66] For example, Retnakumari et al.[67] employed folic acid-conjugated BSA-coated Au_{25} NCs with a maximum emission at 674 nm to specifically target the folate receptor-positive oral carcinoma cells. The labelled cells can be clearly

imaged with the NIR emission. Muhammed et al.[68] used GSH to etch mercaptosuccinic acid-protected AuNPs at pH 7–8 and obtained GSH-coated Au_{23} clusters with NIR emission at 685 nm. After conjugation with streptavidin, these AuNCs could selectively target to human hepatoma cells (HepG2) due to the strong binding between streptavidin and the over-expressed biotin on HepG2 cells. Polavarapu et al.[69] also investigated nanotoxicity of fluorescent AuNCs by incubating SH-SY5Y human neuroblastoma cells with GSH-coated AuNCs with a maximum emission at 780 nm for 24 h (Figure 2a and b). The detailed MTT studies showed that the cells are still viable even after incubated with a concentration of AuNCs up to 400 μg/mL, indicating low cytotoxicity of the luminescent AuNCs.

In addition to conventional one-photon excitation fluorescence imaging, two-photon excitation is a fluorescence imaging technique that allows imaging living tissue at a high-penetration depth and high-spatial resolution because of the tissue scattering and autofluorescence background that are minimized in multiphoton microscopy.[70–72] Ramakrishna et al.[73] studied the two-photon excitation of AuNCs in hexane, showing that the two-photon absorption (TPA) cross sections of Au_{25} and Au_{2406} cluster were 427,000 GM and 3,452,000 GM, respectively. Strong two-photon emission of AuNCs can be also observed in aqueous solution. Polavarapu et al.[69] explored the two-photon emission of GSH-coated AuNCs in water, where the TPA cross section was quantified to be 189,740 GM under 800 nm excitation, several orders higher than most of the currently used organic dyes or QDs. The large TPA of AuNCs further broadens their bioimaging applications. For example, Polavarapu et al.[69] reported the two-photon excitation cell imaging with GSH-coated AuNCs. The SH-SY5Y human neuroblastoma cells can be clearly imaged without auto-fluorescence background under an 800-nm pulse laser excitation (Figure 2c and d). Liu et al.[74] applied dextran-coated 11-mercaptoundecanoic acid (MUA) functionalized-AuNCs to image human mesenchymal stem cells (hMSCs) with two-photon excitation. Dextran polymers are widely used in biomedical and pharmaceutical fields because of their ability to facilitate the internalization of various kinds of biomaterials into tumour cells.[75] Upon 800-nm laser excitation, the hMSCs cells can be successfully imaged based on the emission at 530 nm from the internalized dextran-coated 11-MUA AuNCs.

In vivo fluorescence imaging of few-atom luminescent AuNCs

Not limited to in vitro imaging elaborated above, few-atom fluorescent AuNCs also find applications in animal imaging. Recently, Wu et al.[76] investigated tumour targeting of NIR emitting BSA-stabilized AuNCs. NIR fluorescence of the AuNCs significantly improved tissue penetration depth up to few millimetres. Due to their small hydrodynamic radius (~2.7 nm), injected BSA-coated AuNCs were found to mainly accumulate in liver (29 ± 3.7%), spleen (13 ± 4.4%) and kidneys, which were relatively smaller compared to other NP-based contrast imaging agents. In addition, because of the enhanced permeability and retention effects, these BSA-AuNCs were highly uptaken by the tumours and can be imaged with a distinguishable tumour-to-background ratio (Figure 3).[76]

Few-nanometre luminescent AuNPs

Due to the large density of states and extremely small electron Fermi wavelength (0.5 nm) of gold metal, luminescence of AuNCs is extremely sensitive to the size, in which quantized states rapidly diminish with the increase of the particle size from few atoms to few nanometres.[28] Therefore, AuNCs with few-nm size typically no longer emit fluorescence. However, in the past decade, a large number of few-nm luminescent AuNPs (1.5–3.0 nm) have been developed.[77–84] Different from those few-atom luminescent AuNCs, few-nm luminescent AuNPs generally have two distinct aspects:[43] (i) a relatively large amount of gold atoms in +1 oxidation state (denoted as Au(I) atoms) and (ii) large Stokes shifts (several

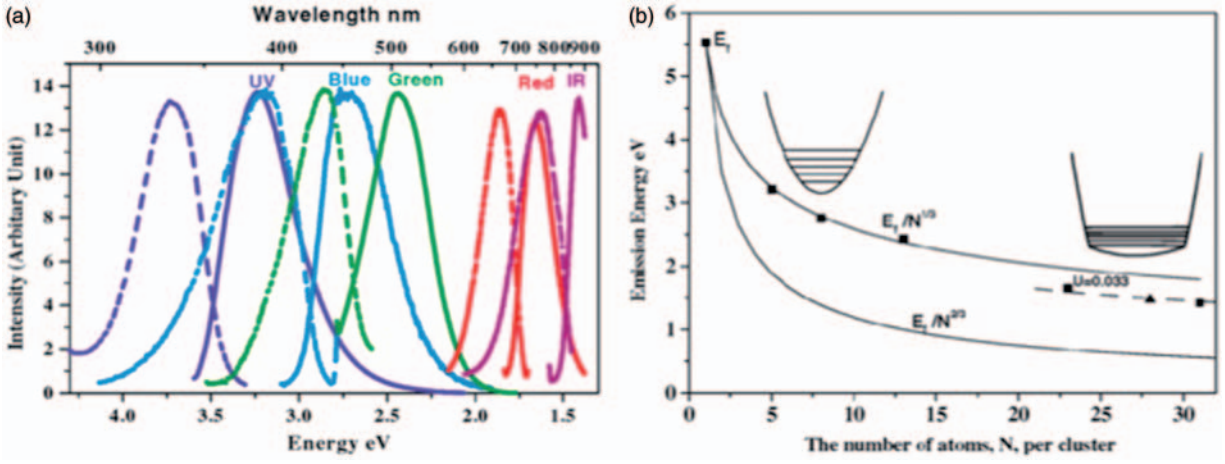

Figure 1 (a) Excitation (dashed) and emission (solid) spectra of different AuNCs. Excitation and emission maxima shift to longer wavelength with the increase of cluster size, suggesting that particle size governs emission from these few-atom luminescent AuNCs; (b) correlation of the number of atoms, N, per cluster with emission energy. Emission energy decreases with increasing number of atoms. The correlation of emission energy with N is quantitatively fit with $E_{Fermi}/N^{1/3}$, as predicted by the spherical jellium model. (Reprinted from Ref. 49, with permission from American Physical Society.) AuNCs: gold nanoclusters. (A colour version of this figure is available in the online journal)

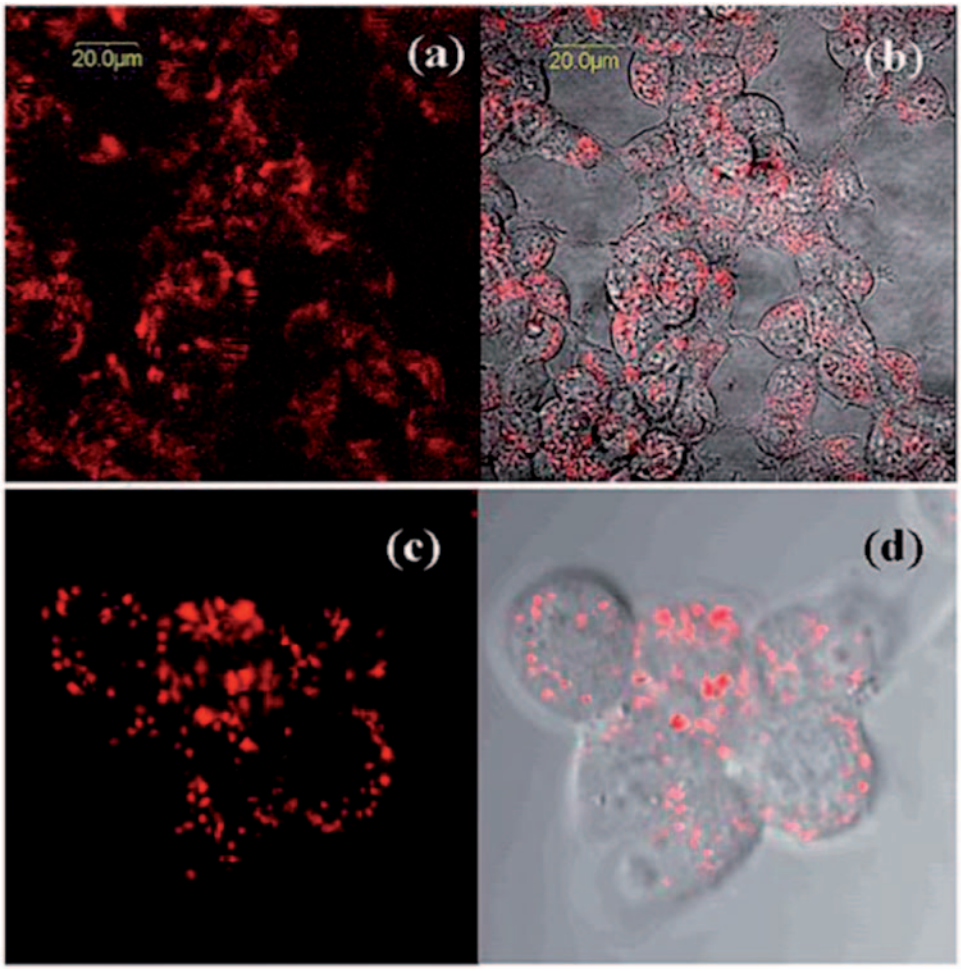

Figure 2 (a) One-photon and (c) two-photon excitation fluorescence images of SH-SY5Y neuroblastoma cells that were incubated with the AuNCs. The images on the right (b and d) are the overlaid pictures of the fluorescence images and the corresponding differential interference contrast (DIC) images. (Reprinted from Ref. 69, with permission from Royal Society of Chemistry.) AuNCs: gold nanoclusters. (A colour version of this figure is available in the online journal)

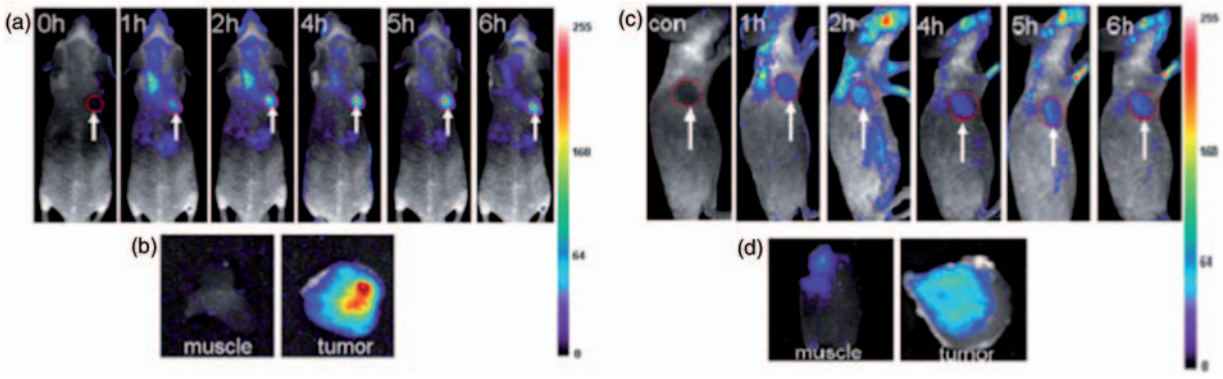

Figure 3 Fluorescence *in vivo* images of mice bearing a (a) MDA-MB-45 tumor and (c) a HeLa tumor after injection of BSA-AuNCs. Strong signal from AuNCs was observed in the tumor (marked by the red circle), demonstrating significant passive accumulation in the tumour by the EPR effect. The arrowheads indicated the tumour. *Ex vivo* fluorescence images of the (b) MDA-MB-45 tumour tissue and (d) HeLa tumour tissue and their comparisons with muscle tissue around the tumour from the mice used in (a) and (c), respectively. (Reprinted from Ref. 76, with permission from Royal Society of Chemistry.) AuNCs: gold nanoclusters; BSA: bovine serum albumin. (A colour version of this figure is available in the online journal)

hundred nanometres) similar to those of luminescent Au(I)-thiol complexes/polynuclear Au(I) clusters where S–Au charge transfer is involved in the emission.

In vitro fluorescence imaging of few-nm luminescent AuNPs

Huang et al.[85] successfully applied thioether-terminated poly(methacrylic acid)-coated luminescent AuNPs with red

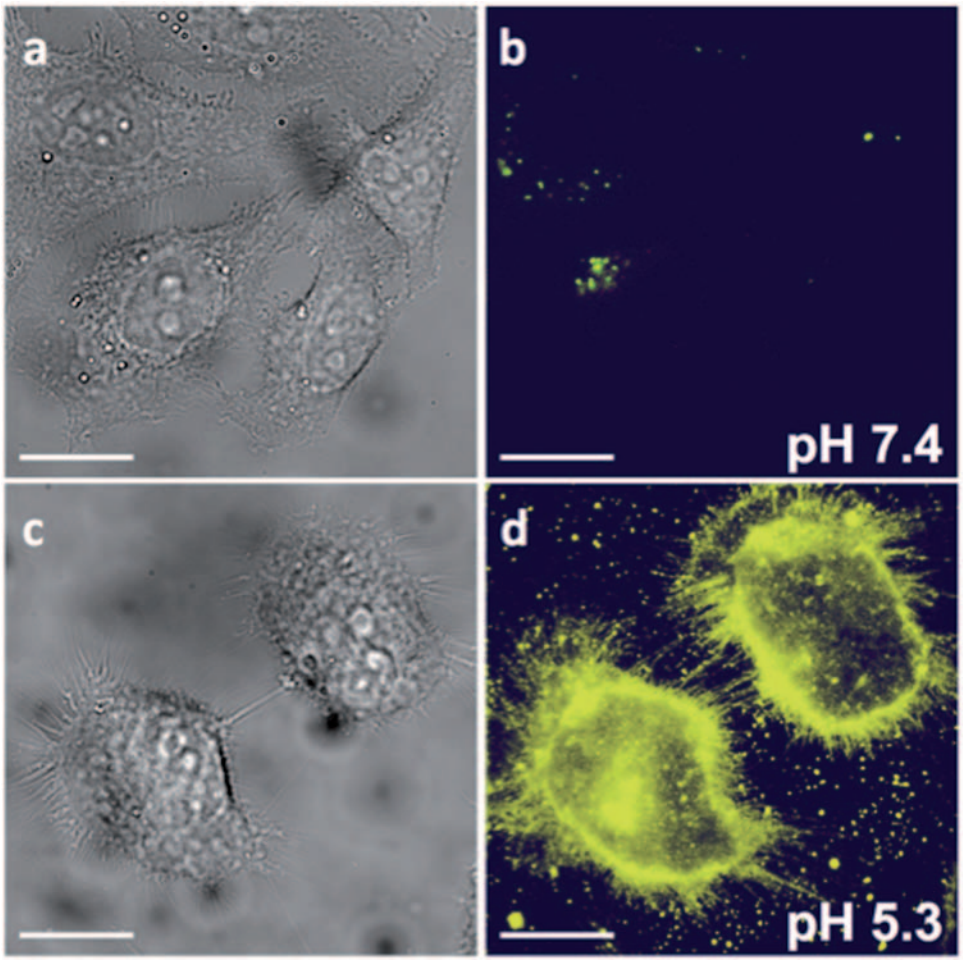

Figure 4 pH-dependent adsorption of luminescent GC-AuNPs on live HeLa cell membrane. Bright field (a, c) and fluorescence (b, d) images of live HeLa cells incubated with 0.2 mg/mL GC-AuNPs at pH 7.4 (a, b) and pH 5.3 (c, d) in PBS at 25°C for 10 min, respectively (scalar bar, 20 μm). (Reprinted from Ref. 89, with permission from American Chemical Society.) (A colour version of this figure is available in the online journal)

emission to image cord blood mononuclear cells and K562 cancer cells after 24-h incubation with these AuNPs in the cell-culture medium. Chou and co-workers used red-emitting insulin-coated AuNPs with maximum emission at 670 nm to serve as a fluorescent biomarker to distinguish the differentiated versus undifferentiated C2C12 mouse myoblasts due to the overexpression of insulin receptors on the differentiated C2C12 but not on the undifferentiated C2C12 cells.[86] By utilizing ferritin-encapsulated luminescent AuNPs, Sun et al.[87] also demonstrated the fluorescence imaging of human colorectal carcinoma cell line Caco-2 by targeting the ferritin receptors on the Caco-2 plasma membrane. In addition, Lin et al.[88] showed that the dihydrolipoic acid-coated few-nm AuNPs (AuNPs@DHLA) with a maximum emission at 674 nm could be used to image the endogenous biotin of HepG2 cells. By further conjugating the streptavidin with AuNPs@DHLA, the streptavidin-conjugated AuNPs@DHLA successfully stained the endogenous biotin of HepG2 cells with high intensity because of the strong binding affinity between streptavidin and biotin.[88]

We recently developed few-nm luminescent AuNPs with pH-dependent cell membrane adsorption.[89] pH is a critical parameter in many biological processes and also an important indicator for disease progression. However, most metal NPs generally are insensitive to extracellular pH in a native biological environment because serum proteins are often adsorbed onto the metal NPs and form protein 'corona', which actually governs the interactions between NPs and the cell membrane.[90–93] In this study, we employed reduced GSH, abundant in the cytoplasm, to minimize protein adsorption on the NPs.[94] The simplest stable aminothiol, cysteamine, was used as surface ligands to grant the particles pH-dependent adsorption onto the live-cell membrane within a biological pH range (5.3–7.4).[89] These glutathione/cysteamine-coated AuNPs (GC-AuNPs) exhibited little interaction with cells at pH 7.4 in phosphate-buffered saline (PBS) (Figure 4a and b). Once the extracellular pH was further dropped to 5.3, luminescence intensities of the cell membranes observed under fluorescence microscope were increased up to 40 times, indicating the significantly increased adsorption of the GC-AuNPs to the cell membrane in a slightly acidic environment (Figure 4c and d). More interestingly, such pH-dependent behavior was well maintained in the presence of serum protein. The reason is attributed to the increment of global charge

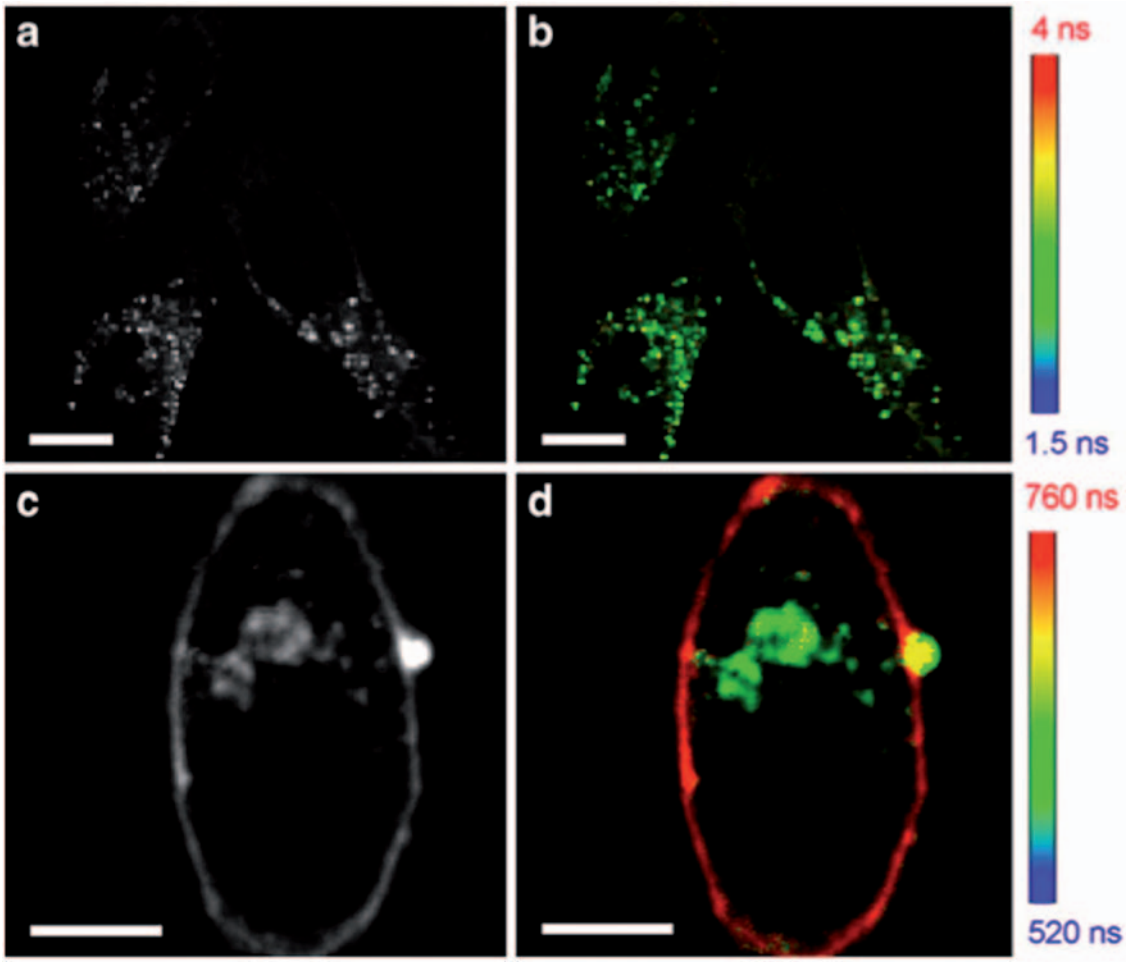

Figure 5 Fluorescence intensity (a, c) and lifetime images (b, d) of HeLa cells only (a and b) and HeLa cells incubated with DHLA-AuNPs (c and d) taken with confocal microscope. (Scale bar: 10 μm). Lifetime maps were calculated by determining the lifetime from the fluorescence decays of all the photon counts registered for each pixel. (Reprinted from Ref. 80, with permission from John Wiley & Sons Inc.) (A colour version of this figure is available in the online journal)

attraction between positively charge cysteamine and negatively charged cell membrane in the acidic environment, whereas glutathione prevents nonspecific protein adsorption.

Similar to few-atom AuNCs, few-nm luminescent AuNPs have been also used for two-photon excitation fluorescence imaging. Nienhaus and co-workers have utilized D-penicillamine-coated few-nm luminescent AuNPs (DPA-AuNPs) for two-photon fluorescence imaging of live HeLa cells under the excitation of an 810-nm laser.[84] A 3D reconstruction of images collected at different z-positions confirmed the internalization of these AuNPs inside the cells as well as adhering to the cell membrane. Specific endocytosis pathways were likely involved in the internalization of DPA-AuNPs because most DPA-AuNPs existed in the form of large aggregates inside the cells. In addition to traditional intensity-based fluorescence imaging, Shang et al.[80] pioneered to utilize the long luminescence lifetime of few-nm AuNPs for cell-imaging application. As shown in Figure 5, long luminescence lifetimes (500–800 ns) were observed inside the cells after incubating NIR emitting DHLA-coated AuNPs with HeLa cells for 1 h, indicating the internalization of these AuNPs by the cells. The obtained fluorescence lifetime images also demonstrated an amplified contrast of DHLA-coated AuNPs in cells, where longer lifetimes were observed from the AuNPs near the cell membrane than those inside the cells, indicating that this technique has potential application in the observation of local microenvironment.

In vivo fluorescence imaging of few-nm luminescent AuNPs

To investigate the possible in vivo application of few-nm luminescent AuNPs, Sun et al.[87] used red-emitting ferritin-encapsulated AuNPs as fluorescence probes for in vivo imaging. After injection of 0.8 nmol/g body weight of the AuNPs throught the tail vein into female nude mice, whole-body fluorescence images were obtained at different time points. Fluorescent signals with a kidney-like shape were observed on each side of the spine 30-min postinjection and reached the highest intensity 3–5 h after injection. The high accumulation of NPs in kidneys observed might be attributed to a specific uptake mechanism related to the certain ferritin receptors in the kidney. Further ex vivo fluorescence imaging and inductively coupled plasma mass spectrometry (ICP-MS) results indicated strong uptake of these AuNPs by liver and spleen with quantitative biodistribution results comparable with those of BSA-coated AuNCs.[76]

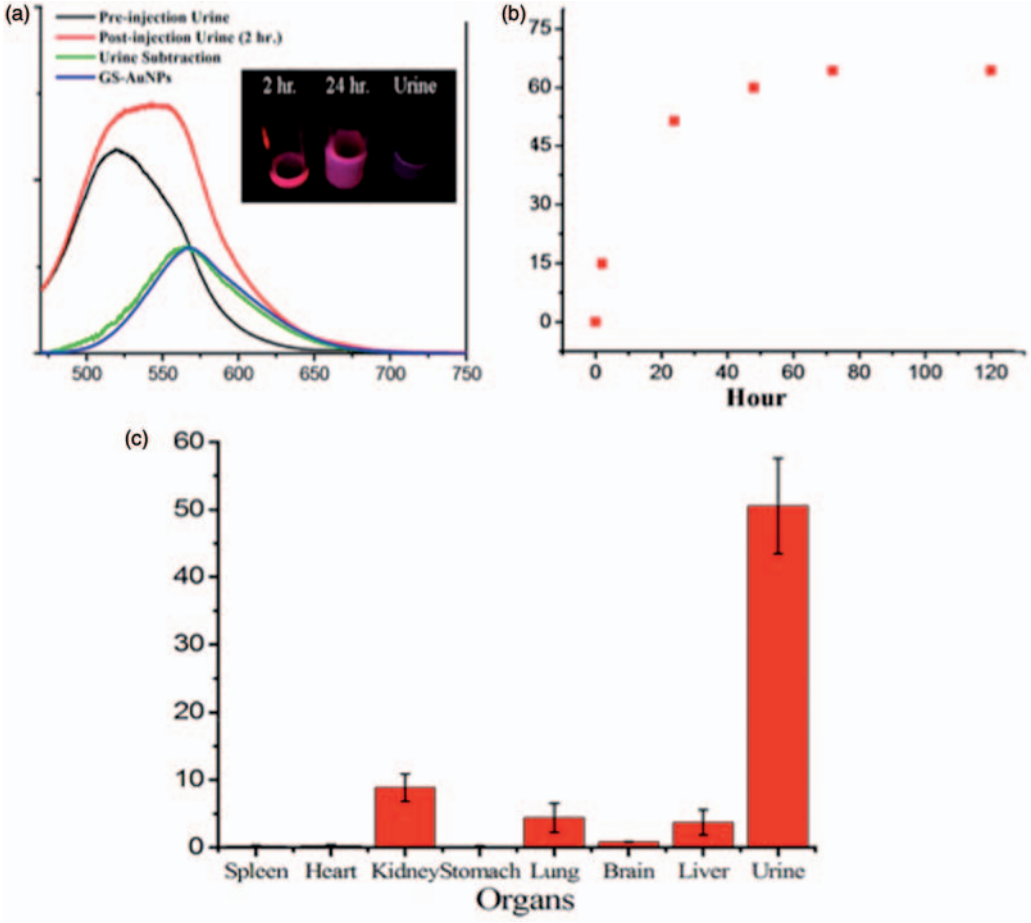

Figure 6 Renal clearance and biodistribution studies of ~2-nm luminescent GS-AuNPs. (a) Luminescence spectra of urine (black), GS-AuNPs (blue), the urine collected 2-h post-injection (p.i.) (red) and the spectrum (green) after subtracting the urine background (excitation at 420 nm). Inset: Luminescence images of GS-AuNPs in the urine at 2 and 24 h p.i. and control urine under excitation with UV light with a 630/75 bandpass filter. (b) Gold concentrations in the urine at 2, 6, 24, 48, 72 and 120 h p.i. measured by ICP-MS. (c) Biodistribution of GS-AuNPs in mice ($n = 3$) 24 h after intravenous injection. The percentage of the injected dose was calculated based on the gold concentration measured by ICP-MS. (Reprinted from Ref. 100, with permission from John Wiley & Sons Inc.) ICP-MS: inductively coupled plasma mass spectrometry; UV: ultraviolet. (A colour version of this figure is available in the online journal)

While most noble metal NPs exhibited strong nonspecific accumulation in reticuloendothelial system (RES) organs after administration, ideal nanomaterial-based imaging agents for in vivo studies should be effectively cleared out of the body and have little accumulation in healthy organs to minimize the nanotoxicity.[95–98] Thus, it is vitally important to develop luminescent AuNPs with efficient clearance profile for future clinical applications. Although NPs with hydrodynamic diameters smaller than ~5.5 nm are generally considered to be stealthy to the RES organs and can be cleared out from the body,[98] particle size is not the only parameter that governs the renal clearance of the particles. For example, ~1.4 nm AuNPs coated by bis(p-sulfonatophenyl)phenylphosphine still severely sequestered in RES.[99] Recently, we discovered that ~2-nm GSH-coated luminescent AuNPs (GS-AuNPs) can be efficiently cleared out of body through urinary system, which is nearly 10–100 times better than those of the similar-sized AuNPs (Figure 6).[100] Such behaviour can be ascribed to both the very small particle size and low affinities to serum protein.[89,94] The fluorescence property of these GS-AuNPs also allowed us to investigate their physiological stability and renal clearance kinetics. Strong luminescence was observed from the urine 2-h postinjection, which was identical to the GS-AuNPs solution in PBS (Figure 6a), further indicating that the luminescent GS-AuNPs were renal clearable and highly stable during body-internal-circulation.[100] ICP-MS results justified that more than 50% of the GS-AuNPs were excreted out of the body within 24 h p.i. and up to 65% after 72 h p.i. (Figure 6b), while only $3.7 \pm 1.9\%$ and $0.3 \pm 0.1\%$ of the GS-AuNPs were accumulated in the liver and spleen, respectively (Figure 6c), remarkably different from those of NPs accumulated in the hepatic route, including similar-sized AuNPs with other ligands,[76,99,100] such as BSA, bis(p-sulfonatophenyl)-phenylphosphine, citrate and cysteamine, providing important foundation for the future development of few-nm luminescent AuNPs. More recently, we further examined the pharmacokinetics of the radioactive NIR-emitting GS-AuNPs, which exhibited a small-molecule-like pharmacokinetics after systemic administration with a distribution half-life ($t_{1/2\alpha}$) of 5.0 min and elimination half-life ($t_{1/2\beta}$) of 12.7 h.[101] The bright NIR-emitting fluorescence and the radioactive gamma emission from ^{198}Au render these GS-[^{198}Au]AuNPs

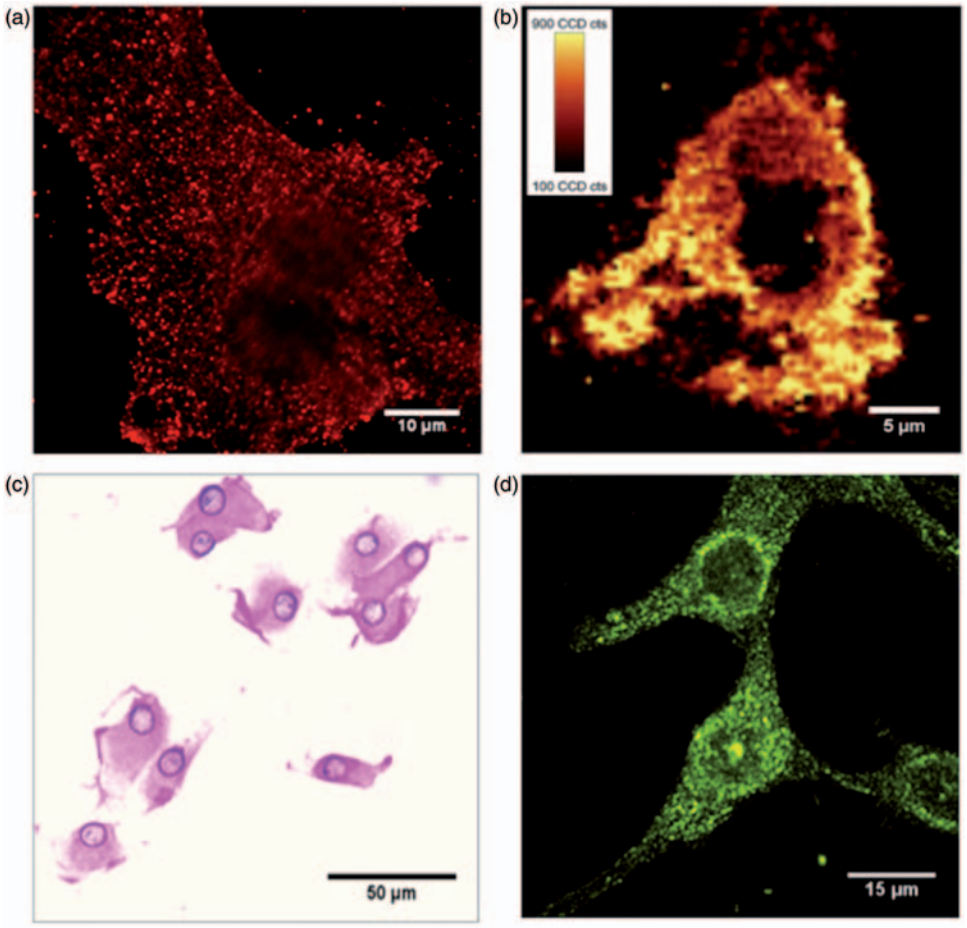

Figure 7 MBA–pAuNPs–cRGD served as a multimodality probe that enables $\alpha_v\beta_3$ integrin receptors on U87MG cancer cells to be imaged with four different imaging techniques at the single-cell level. (a) Strong single particle luminescence from pAuNPs enabled the integrin receptors on a single U87MG cell to be imaged using fluorescence microscopic imaging modality. (b) Raman image of a U87MG cancer cell labelled by MBA–pAuNPs–cRGD, which was constructed based on the Raman vibration of MBA at $1579 \pm 10\,cm^{-1}$ (fluorescence background was subtracted). (c) Bright-field image of the cancer cells labelled by the NPs. Strong surface plasmons of the pAuNPs made the cells purplish. (d) Strong surface plasmon scattering of pAuNPs allows the cancer cells to be visualized using dark-field imaging modality. (Reprinted from Ref. 102, with permission from Royal Society of Chemistry.) MBA: mercaptobenzoic acid; NPs: nanoparticles; pAuNPs: polycrystalline AuNPs. (A colour version of this figure is available in the online journal)

with potential applications as dual-modality imaging probes for the strength integration of both fluorescence and single photon emission computed tomography imaging techniques.

Plasmonic luminescent AuNPs

While tuning particle size and valence state of gold atoms allow us to create a variety of molecular luminescent AuNPs with few-nm sizes, no surface plasmons were observed from these NPs because of the limited number of free electrons.[40,43] Thus, the integration of fluorescence properties into plasmonic AuNPs is of importance in developing multimodality imaging probes. By tuning grain size of a polycrystalline AuNP, we successfully created ~20-nm plasmonic luminescent AuNPs.[102] These plasmonic luminescent AuNPs were synthesized in solid state through thermal reduction of gold–glycine complex and exhibited highly polycrystalline structures with grain size down to 1 nm (denoted as polycrystalline AuNPs; pAuNPs). Different from conventional plasmonic AuNPs that were often nonfluorescent, the co-existence of continuous electron band and discrete energy states within one single NP results in strong single-particle emission due to the coupling between surface plasmons and luminescence within a single particle.[102] In addition to the thermal reduction method, Gaiduk et al.[103] used a high-energy pulsed laser to convert nonluminescent 20 nm AuNPs into emissive ones with a quantum yield of $\sim 1.4 \times 10^{-6}$. However, the limitation of this method is that no enough plasmonic luminescent AuNPs are generated, limiting their practical applications.

Imaging applications of plasmonic luminescent AuNPs

While the in vivo behaviour of plasmonic luminescent AuNPs remained little known due to the limited reported studies, the current explorations on imaging applications of pAuNPs mainly focused on in vitro cellular level. Recently, we employed pAuNPs to demonstrate their applications as a multimodal nanoprobe for optical microscopic imaging of U87MG cancer cells based on their both fluorescence and plasmonic properties.[102] After conjugation with a Raman

tag mercaptobenzoic acid (MBA) and thiolated Cyclic Arg-Gly-Asp (cRGD) peptide, a specific peptide exhibits high-binding affinity (IC50 = ~8 nM) to $\alpha_v\beta_3$ integrin receptors on U87MG cancer cells,[34] the cells labelled with MBA–pAuNPs–cRGD can be imaged with four different imaging techniques (Figure 7). Under mercury-lamp excitation, the diffraction-limited fluorescence spots of MBA–pAuNPs–cRGD can be readily observed on the U87MG cell membrane under fluorescence microscopy (Figure 7a). The blinking/intensity fluctuation was also observed, indicating that the majority of the NPs were monodispersed on the cell membrane while they were bound to the receptors. In addition to fluorescence imaging, the plasmonic properties of pAuNPs also enabled us to more readily image cancer cells with other optical microscopies. For example, the SERS image of labelled U87MG cells can be constructed by utilizing the characteristic vibrations of MBA at $1579 \pm 10\,cm^{-1}$ (Figure 7b) using a confocal scanning Raman microscope. Chemical imaging of targeting molecule cRGD peptide can be also achieved with the strong SERS signal containing characteristic vibrations of both cRGD peptide and MBA. Strong surface plasmon absorption of MBA–pAuNPs–cRGD resulted in pink colour of the labelled U87MG cells and can be observed even with naked eyes (Figure 7c), which offered a simple way for the detection of cRGD receptors. The large surface plasmon scattering from MBA–pAuNPs–cRGD also allowed us to image these cancer cells with a dark-field imaging technique at the single particle level (Figure 7d). With the integrated and enhanced plasmonic and luminescence properties, these pAuNPs are expected to further help unravel cellular structures with chemical information at a high spatial and temporal resolution in the future.

In addition to bioimaging applications we demonstrated, He et al.[104] showed that plasmonic luminescent AuNPs of 38 nm can be internalized by the HeLa cells and accumulated inside the cytoplasm of these cells.

Summary and future prospects

After one-decade's efforts, the synthesis of luminescent AuNPs is no longer a challenge. Luminescent AuNPs with different sizes and surface chemistries have been successfully created. In this minireview, we briefly summarized the recent advances in bioimaging applications of different-sized luminescent AuNPs at both in vitro and in vivo levels. As we can see, the great potential of luminescent metal NPs has not been fully explored. Therefore, it is predicable that the future of luminescent metal NPs will mainly focus on their biomedical applications due to their biocompatibility and physiological stabilities. For example, since intrinsic emission arising from AuNPs rather than the surface ligands, we can use them to probe the interactions between surface ligands and cell membranes. Multimodality of plasmonic luminescent AuNPs will allow us to unravel chemical interactions involved in the internalization of AuNPs. The efficient renal clearance of luminescent AuNPs might lead to the development of a new generation of multimodal probes for clinical cancer imaging with low toxicity. With these unique merits of luminescent metal NPs, we have no doubt that luminescent metal NPs can serve as a new generation of nanoprobes to address many challenges in the fundamental understanding of cell biology and clinical disease diagnosis that current probes might not easily tackle.

Author contributions: All authors contributed to writing and proofreading of this review.

ACKNOWLEDGEMENTS

This work is supported in part by NIH (R21EB009853 and 1R21EB011762), CPRIT (RP120588) and the start-up fund from the University of Texas at Dallas.

REFERENCES

1. Murphy DB. Fundamentals of Light Microscopy and Electronic Imaging. 1st ed. New York: Wiley-Liss, 2001
2. Massoud TF, Gambhir SS. Molecular imaging in living subjects: seeing fundamental biological processes in a new light. Gene Dev 2003;17:545–80
3. Zipfel WR, Williams RM, Webb WW. Nonlinear magic: multiphoton microscopy in the biosciences. Nat Biotechnol 2003;21:1369–77
4. Yildiz A, Selvin PR. Fluorescence imaging with one manometer accuracy: application to molecular motors. Acc Chem Res 2005;38:574–82
5. Lichtman JW, Conchello JA. Fluorescence microscopy. Nat Methods 2005;2:910–9
6. Huang B, Bates M, Zhuang XW. Super-resolution fluorescence microscopy. Annu Rev Biochem 2009;78:993–1016
7. Bruchez M, Moronne M, Gin P, Weiss S, Alivisatos AP. Semiconductor nanocrystals as fluorescent biological labels. Science 1998;281:2013–6
8. Zhang J, Campbell RE, Ting AY, Tsien RY. Creating new fluorescent probes for cell biology. Nat Rev Mol Cell Biol 2002;3:906–18
9. Gao XH, Cui YY, Levenson RM, Chung LWK, Nie SM. In vivo cancer targeting and imaging with semiconductor quantum dots. Nat Biotechnol 2004;22:969–76
10. Haugland RP. The Handbook—A Guide to Fluorescent Probes and Labeling Technologies. New York: Invitrogen Corp., 2005
11. Michalet X, Pinaud FF, Bentolila LA, Tsay JM, Doose S, Li JJ, Sundaresan G, Wu AM, Gambhir SS, Weiss S. Quantum dots for live cells, in vivo imaging, and diagnostics. Science 2005;307:538–44
12. Giepmans BNG, Adams SR, Ellisman MH, Tsien RY. Review—the fluorescent toolbox for assessing protein location and function. Science 2006;312:217–24
13. Resch-Genger U, Grabolle M, Cavaliere-Jaricot S, Nitschke R, Nann T. Quantum dots versus organic dyes as fluorescent labels. Nat Methods 2008;5:763–75
14. Mishra A, Behera RK, Behera PK, Mishra BK, Behera GB. Cyanines during the 1990s: a review. Chem Rev 2000;100:1973–2011
15. Sameiro M, Goncalves T. Fluorescent labeling of biomolecules with organic probes. Chem Rev 2009;109:190–212
16. Giuliano KA, Post PL, Hahn KM, Taylor DL. Fluorescent protein biosensors—measurement of molecular-dynamics in living cells. Annu Rev Biophys Biomol Struct 1995;24:405–34
17. Yildiz A, Forkey JN, McKinney SA, Ha T, Goldman YE, Selvin PR. Myosin V walks hand-over-hand: single fluorophore imaging with 1.5-nm localization. Science 2003;300:2061–5
18. Citrin D, Lee AK, Scott T, Sproull M, Menard C, Tofilon PJ, Camphausen K. In vivo tumor imaging in mice with near-infrared labeled endostatin. Mol Cancer Ther 2004;3:481–8
19. Chen XY, Conti PS, Moats RA. In vivo near-infrared fluorescence imaging of integrin alpha(v)beta(3) in brain tumor xenografts. Cancer Res 2004;64:8009–14
20. Luo S, Zhang E, Su Y, Cheng T, Shi C. A review of NIR dyes in cancer targeting and imaging. Biomaterials 2011;32:7127–38
21. Tanaka E, Choi HS, Fujii H, Bawendi MG, Frangioni JV. Image-guided oncologic surgery using invisible light: completed pre-clinical development for sentinel lymph node mapping. Ann Surg Oncol 2006;13:1671–81

22. Fernandez-Suarez M, Ting AY. Fluorescent probes for super-resolution imaging in living cells. Nat Rev Mol Cell Biol 2008;9:929–43
23. Chalfie M, Tu Y, Euskirchen G, Ward WW, Prasher DC. Green fluorescent proteins as a marker for gene-expression. Science 1994;263:802–5
24. Tsien RY. The green fluorescent protein. Annu Rev Biochem 1998;67:509–44
25. Gronemeyer T, Godin G, Johnsson K. Adding value to fusion proteins through covalent labelling. Curr Opin Biotechnol 2005;16:453–8
26. Miller LW, Cornish VW. Selective chemical labeling of proteins in living cells. Curr Opin Chem Biol 2005;9:56–61
27. Betzig E, Patterson GH, Sougrat R, Lindwasser OW, Olenych S, Bonifacino JS, Davidson MW, Lippincott-Schwartz J, Hess HF. Imaging intracellular fluorescent proteins at nanometer resolution. Science 2006;313:1642–5
28. Alivisatos AP. Semiconductor clusters, nanocrystals, and quantum dots. Science 1996;271:933–7
29. Gao XH, Yang LL, Petros JA, Marshal FF, Simons JW, Nie SM. In vivo molecular and cellular imaging with quantum dots. Curr Opin Biotechnol 2005;16:63–72
30. Chan WCW, Maxwell DJ, Gao XH, Bailey RE, Han MY, Nie SM. Luminescent quantum dots for multiplexed biological detection and imaging. Curr Opin Biotechnol 2002;13:40–6
31. Jaiswal JK, Mattoussi H, Mauro JM, Simon SM. Long-term multiple color imaging of live cells using quantum dot bioconjugates. Nat Biotechnol 2003;21:47–51
32. Larson DR, Zipfel WR, Williams RM, Clark SW, Bruchez MP, Wise FW, Webb WW. Water-soluble quantum dots for multiphoton fluorescence imaging in vivo. Science 2003;300:1434–6
33. Medintz IL, Uyeda HT, Goldman ER, Mattoussi H. Quantum dot bioconjugates for imaging, labelling and sensing. Nat Mater 2005;4:435–46
34. Cai WB, Chen XY. Preparation of peptide-conjugated quantum dots for tumor vasculature-targeted imaging. Nat Protoc 2008;3:89–96
35. Derfus AM, Chan WCW, Bhatia SN. Probing the cytotoxicity of semiconductor quantum dots. Nano Lett 2004;4:11–8
36. Hoshino A, Fujioka K, Oku T, Suga M, Sasaki YF, Ohta T, Yasuhara M, Suzuki K, Yamamoto K. Physicochemical properties and cellular toxicity of nanocrystal quantum dots depend on their surface modification. Nano Lett 2004;4:2163–9
37. Oberdorster G, Oberdorster E, Oberdorster J. Nanotoxicology: An emerging discipline evolving from studies of ultrafine particles. Environ Health Perspect 2005;113:823–39
38. Baker M. Nanotechnology imaging probes: smaller and more stable. Nat Methods 2010;7:957–62
39. Ashcroft NW, Mermin ND. Solid State Physics. New York: HOLT, Rinehart and Winston, 1976
40. Zheng J, Nicovich PR, Dickson RM. Highly fluorescent noble-metal quantum dots. Annu Rev Phys Chem 2007;58:409–31
41. Shang L, Dong S, Nienhaus GU. Ultra-small fluorescent metal nanoclusters: synthesis and biological applications. Nano Today 2011;6:401–18
42. Lin CAJ, Lee CH, Hsieh JT, Wang HH, Li JK, Shen JL, Chan WH, Yeh HI, Chang WH. Synthesis of fluorescent metallic nanoclusters toward biomedical application: recent progress and present challenges. J Med Biol Eng 2009;29:276–83
43. Zheng J, Zhou C, Yu MX, Liu JB. Different sized luminescent gold nanoparticles. Nanoscale 2012;4:4073–83
44. Kreibig U, Vollmer M. Optical Properties of Metal Clusters. New York: Springer, 1995
45. Kubo R. Electronic properties of metallic fine particles. J Phys Soc Jpn 1962;17:975
46. Schaaff TG, Shafigullin MN, Khoury JT, Vezmar I, Whetten RL, Cullen WG, First PN. Isolation of smaller nanocrystal au molecules: robust quantum effects in optical spectra. J Phys Chem B 1997;101:7885–91
47. Sanchez A, Abbet S, Heiz U, Schneider WD, Häkkinen H, Barnett RN, Landman U. When gold is not noble: nanoscale gold catalysts. J Phys Chem A 1999;103:9573–8
48. Wallace WT, Whetten RL. Coadsorption of CO and O_2 on selected gold clusters: evidence for efficient room-temperature CO_2 generation. J Am Chem Soc 2002;124:7499–505
49. Zheng J, Zhang C, Dickson RM. Highly fluorescent, water-soluble, size-tunable gold quantum dots. Phys Rev Lett 2004;93:077402
50. Esumi K, Suzuki A, Yamahira A, Torigoe K. Role of poly(amidoamine) dendrimers for preparing nanoparticles of gold, platinum, and silver. Langmuir 2000;16:2604–8
51. Zheng J, Petty JT, Dickson RM. High quantum yield blue emission from water-soluble Au-8 nanodots. J Am Chem Soc 2003;125:7780–1
52. Knight WD, Clemenger K, Deheer WA, Saunders WA, Chou MY, Cohen ML. Electronic shell structure and abundances of sodium clusters. Phys Rev Lett 1984;52:2141–3
53. Deheer WA, Selby K, Kresin V, Masui J, Vollmer M, Chatelain A, Knight WD. Collective dipole oscillations in small sodium clusters. Phys Rev Lett 1987;59:1805–8
54. Deheer WA. The physics of simple metal-clusters—experimental aspects and simple-models. Rev Mod Phys 1993;65:611–76
55. Link S, Beeby A, FitzGerald S, El-Sayed MA, Schaaff TG, Whetten RL. Visible to infrared luminescence from a 28-atom gold cluster. J Phys Chem B 2002;106:3410–5
56. Jin RC, Egusa S, Scherer NF. Thermally-induced formation of atomic Au clusters and conversion into nanocubes. J Am Chem Soc 2004;126:9900–1
57. Duan HW, Nie SM. Etching colloidal gold nanocrystals with hyperbranched and multivalent polymers: a new route to fluorescent and water-soluble atomic clusters. J Am Chem Soc 2007;129:2412
58. Xie JP, Zheng YG, Ying JY. Protein-directed synthesis of highly fluorescent gold nanoclusters. J Am Chem Soc 2009;131:888
59. Zhou RJ, Shi MM, Chen XQ, Wang M, Chen HZ. Atomically monodispersed and fluorescent sub-nanometer gold clusters created by biomolecule-assisted etching of nanometer-sized gold particles and rods. Chem Eur J 2009;15:4944–51
60. Muhammed MAH, Verma PK, Pal SK, Retnakumari A, Koyakutty M, Nair S, Pradeep T. Luminescent quantum clusters of gold in bulk by albumin-induced core etching of nanoparticles: metal ion sensing, metal-enhanced luminescence, and biolabeling. Chem Eur J 2010;16:10103–12
61. Gonzalez BS, Rodriguez MJ, Blanco C, Rivas J, Lopez-Quintela MA, Martinho JMG. One step synthesis of the smallest photo luminescent and paramagnetic PVP-protected gold atomic clusters. Nano Lett 2010;10:4217–21
62. Kawasaki H, Hamaguchi K, Osaka I, Arakawa R. ph-Dependent synthesis of pepsin-mediated gold nanoclusters with blue green and red fluorescent emission. Adv Funct Mater 2011;21:3508–15
63. Lin SY, Chen NT, Sum SP, Lo LW, Yang CS. Ligand exchanged photoluminescent gold quantum dots functionalized with leading peptides for nuclear targeting and intracellular imaging. Chem Commun 2008;4762–4
64. Jao YC, Chen MK, Lin SY. Enhanced quantum yield of dendrimer-entrapped gold nanodots by a specific ion-pair association and microwave irradiation for bioimaging. Chem Commun 2010;46:2626–8
65. Weissleder R, Ntziachristos V. Shedding light onto live molecular targets. Nat Med 2003;9:123–8
66. Frangioni JV. In vivo near-infrared fluorescence imaging. Curr Opin Chem Biol 2003;7:626–34
67. Retnakumari A, Setua S, Menon D, Ravindran P, Muhammed H, Pradeep T, Nair S, Koyakutty M. Molecular-receptor-specific, non-toxic, near-infrared-emitting Au cluster-protein nanoconjugates for targeted cancer imaging. Nanotechnology 2010;21:055103
68. Muhammed MAH, Verma PK, Pal SK, Kumar RCA, Paul S, Omkumar RV, Pradeep T. Bright, NIR-emitting Au-23 from Au-25: characterization and applications including biolabeling. Chem Eur J 2009;15:10110–20
69. Polavarapu L, Manna M, Xu QH. Biocompatible glutathione capped gold clusters as one- and two-photon excitation fluorescence contrast agents for live cells imaging. Nanoscale 2011;3:429–34
70. Xu C, Zipfel W, Shear JB, Williams RM, Webb WW. Multiphoton fluorescence excitation: new spectral windows for biological nonlinear microscopy. Proc Natl Acad Sci USA 1996;93:10763–8
71. Helmchen F, Denk W. Deep tissue two-photon microscopy. Nat Methods 2005;2:932–40

72. So PTC, Dong CY, Masters BR, Berland KM. Two-photon excitation fluorescence microscopy. Annu Rev Biomed Eng 2000;2:399–429
73. Ramakrishna G, Varnavski O, Kim J, Lee D, Goodson T. Quantum-sized gold clusters as efficient two-photon absorbers. J Am Chem Soc 2008;130:5032
74. Liu CL, Ho ML, Chen YC, Hsieh CC, Lin YC, Wang YH, Yang MJ, Duan HS, Chen BS, Lee JF, Hsiao JK, Chou PT. Thiol-functionalized gold nanodots: two-photon absorption property and imaging in vitro. J Phys Chem C 2009;113:21082–9
75. Vittorio O, Cirillo G, Iemma F, Di Turi G, Jacchetti E, Curcio M, Barbuti S, Funel N, Parisi OI, Puoci F, Picci N. Dextran-catechin conjugate: a potential treatment against the pancreatic ductal adenocarcinoma. Pharm Res 2012;29:2601–14
76. Wu X, He XX, Wang KM, Xie C, Zhou B, Qing ZH. Ultrasmall near-infrared gold nanoclusters for tumor fluorescence imaging in vivo. Nanoscale 2010;2:2244–9
77. Wang GL, Huang T, Murray RW, Menard L, Nuzzo RG. Near-IR luminescence of monolayer-protected metal clusters. J Am Chem Soc 2005;127:812–3
78. Zhou C, Sun C, Yu MX, Qin YP, Wang JG, Kim M, Zheng J. Luminescent gold nanoparticles with mixed valence states generated from dissociation of polymeric Au(I) thiolates. J Phys Chem C 2010;114:7727–32
79. Tang Z, Robinson DA, Bokossa N, Xu B, Wang S, Wang G. Mixed dithiolate durene-DT and monothiolate phenylethanethiolate protected Au-130 nanoparticles with discrete core and core-ligand energy states. J Am Chem Soc 2011;133:16037–44
80. Shang L, Azadfar N, Stockmar F, Send W, Trouillet V, Bruns M, Gerthsen D, Nienhaus GU. One-pot synthesis of near-infrared fluorescent gold clusters for cellular fluorescence lifetime imaging. Small 2011;7:2614–20
81. Tu XJ, Chen WB, Guo XQ. Facile one-pot synthesis of near-infrared luminescent gold nanoparticles for sensing copper (II). Nanotechnology 2011;22:095701
82. Huang CC, Yang Z, Lee KH, Chang HT. Synthesis of highly fluorescent gold nanoparticles for sensing mercury(II). Angew Chem Int Ed 2007;46:6824–8
83. Guo YM, Wang Z, Shao HW, Jiang XY. Stable fluorescent gold nanoparticles for detection of Cu^{2+} with good sensitivity and selectivity. Analyst 2012;137:301–4
84. Shang L, Dorlich RM, Brandholt S, Schneider R, Trouillet V, Bruns M, Gerthsen D, Nienhaus GU. Facile preparation of water-soluble fluorescent gold nanoclusters for cellular imaging applications. Nanoscale 2011;3:2009–14
85. Huang X, Luo Y, Li Z, Li BY, Zhang H, Li L, Majeed I, Zou P, Tan B. Biolabeling hematopoietic system cells using near-infrared fluorescent gold nanoclusters. J Phys Chem C 2011;115:16753–63
86. Liu CL, Wu HT, Hsiao YH, Lai CW, Shih CW, Peng YK, Tang KC, Chang HW, Chien YC, Hsiao JK, Cheng JT, Chou PT. Insulin-directed synthesis of fluorescent gold nanoclusters: preservation of insulin bioactivity and versatility in cell imaging. Angew Chem Int Ed 2011;50:7056–60
87. Sun CJ, Yang H, Yuan Y, Tian X, Wang LM, Guo Y, Xu L, Lei JL, Gao N, Anderson GJ, Liang XJ, Chen CY, Zhao YL, Nie GJ. Controlling assembly of paired gold clusters within apoferritin nanoreactor for in vivo kidney targeting and biomedical imaging. J Am Chem Soc 2011;133:8617–24
88. Lin C-AJ, Yang T-Y, Lee C-H, Huang SH, Sperling RA, Zanella M, Li JK, Shen JL, Wang HH, Yeh HI, Parak WJ, Chang WH. Synthesis, characterization, and bioconjugation of fluorescent gold nanoclusters toward biological labeling applications. ACS Nano 2009;3:395–401
89. Yu MX, Zhou C, Liu JB, Hankins JD, Zheng J. Luminescent gold nanoparticles with pH-dependent membrane adsorption. J Am Chem Soc 2011;133:11014–7
90. Lynch I, Dawson KA. Protein-nanoparticle interactions. Nano Today 2008;3:40–7
91. Rocker C, Potzl M, Zhang F, Parak WJ, Nienhaus GU. A quantitative fluorescence study of protein monolayer formation on colloidal nanoparticles. Nat Nanotechnol 2009;4:577–80
92. Vincent A, Babu S, Heckert E, Dowding J, Hirst SM, Inerbaev TM, Self WT, Reilly CM, Masunov AE, Rahman TS, Seal S. Protonated nanoparticle surface governing ligand tethering and cellular targeting. ACS Nano 2009;3:1203–11
93. Patil S, Sandberg A, Heckert E, Self WT, Seal S. Protein adsorption and cellular uptake of cerium oxide nanoparticles as a function of zeta potential. Biomaterials 2007;28:4600–7
94. Rosi NL, Giljohann DA, Thaxton CS, Lytton-Jean AKR, Han MS, Mirkin CA. Oligonucleotide-modified gold nanoparticles for intracellular gene regulation. Science 2006;312:1027–30
95. Nel A, Xia T, Madler L, Li N. Toxic potential of materials at the nanolevel. Science 2006;311:622–7
96. Liu WH, Choi HS, Zimmer JP, Tanaka E, Frangioni JV, Bawendi M. Compact cysteine-coated CdSe(ZnCdS) quantum dots for in vivo applications. J Am Chem Soc 2007;129:14530
97. Longmire M, Choyke PL, Kobayashi H. Clearance properties of nanosized particles and molecules as imaging agents: considerations and caveats. Nanomedicine-UK 2008;3:703–17
98. Choi HS, Liu WH, Liu FB, Nasr K, Misra P, Bawendi MG, Frangioni JV. Design considerations for tumour-targeted nanoparticles. Nat Nanotechnol 2010;5:42–7
99. Semmler-Behnke M, Kreyling WG, Lipka J, Fertsch S, Wenk A, Takenaka S, Schmid G, Brandau W. Biodistribution of 1.4-and 18-nm gold particles in rats. Small 2008;4:2108–11
100. Zhou C, Long M, Qin YP, Sun XK, Zheng J. Luminescent gold nanoparticles with efficient renal clearance. Angew Chem Int Ed 2011;50:3168–72
101. Zhou C, Hao GY, Thomas P, Liu JB, Yu MX, Sun SS, Öz OK, Sun XK, Zheng J. Near infrared emitting radioactive gold nanoparticles with small-molecule-like pharmacokinetics. Angew Chem Int Ed 2012;51:10118–22
102. Zhou C, Yu J, Qin YP, Zheng J. Grain size effects in polycrystalline gold nanoparticles. Nanoscale 2012;4:4228–33
103. Gaiduk A, Yorulmaz M, Orrit M. Correlated absorption and photoluminescence of single gold nanoparticles. Chemphyschem 2011;12:1536–41
104. He H, Xie C, Ren J. Nonbleaching fluorescence of gold nanoparticles and its applications in cancer cell imaging. Anal Chem 2008;80:5951–7